



**HAL**  
open science

## Microkinetic Modeling of Acetylene Hydrogenation Under Periodic Reactor Operation

Caroline Urmès, Cécile Daniel, Jean-Marc Schweitzer, Amandine Cablac,  
Carine Julcour-Lebigue, Y. Schuurman

► **To cite this version:**

Caroline Urmès, Cécile Daniel, Jean-Marc Schweitzer, Amandine Cablac, Carine Julcour-Lebigue, et al.. Microkinetic Modeling of Acetylene Hydrogenation Under Periodic Reactor Operation. *Chem-CatChem*, 2022, 14 (8), pp.e202101826. 10.1002/cctc.202101826 . hal-03618515

**HAL Id: hal-03618515**

**<https://hal.science/hal-03618515>**

Submitted on 4 Jul 2022

**HAL** is a multi-disciplinary open access archive for the deposit and dissemination of scientific research documents, whether they are published or not. The documents may come from teaching and research institutions in France or abroad, or from public or private research centers.

L'archive ouverte pluridisciplinaire **HAL**, est destinée au dépôt et à la diffusion de documents scientifiques de niveau recherche, publiés ou non, émanant des établissements d'enseignement et de recherche français ou étrangers, des laboratoires publics ou privés.



## Open Archive Toulouse Archive Ouverte (OATAO)

OATAO is an open access repository that collects the work of Toulouse researchers and makes it freely available over the web where possible

This is an author's version published in: <http://oatao.univ-toulouse.fr/29104>

**Official URL:** <https://doi.org/10.1002/cctc.202101826>

**To cite this version:**

Urmès, Caroline and Daniel, Cécile and Schweitzer, Jean-Marc and Cabiac, Amandine and Julcour-Lebigue, Carine  and Schuurman, Yves *Microkinetic Modeling of Acetylene Hydrogenation Under Periodic Reactor Operation*. (2022) ChemCatChem, 14 (8). e202101826. ISSN 1867-3880

Any correspondence concerning this service should be sent to the repository administrator: [tech-oatao@listes-diff.inp-toulouse.fr](mailto:tech-oatao@listes-diff.inp-toulouse.fr)

# Microkinetic Modeling of Acetylene Hydrogenation Under Periodic Reactor Operation

Caroline Urmès,<sup>[a, b]</sup> Cécile Daniel,<sup>[a]</sup> Jean-Marc Schweitzer,<sup>[b]</sup> Amandine Cabiac,<sup>[b]</sup>  
Carine Julcour,<sup>[c]</sup> and Yves Schuurman<sup>\*[a]</sup>

Dynamic reactor operations will gain interest with the increase of intermittent electricity from renewable sources. Periodic operation of catalytic reactors can also be used for kinetic studies with better parameter estimation than steady-state operation. This methodology is exemplified for the case of acetylene hydrogenation over Pd/ $\alpha$ -Al<sub>2</sub>O<sub>3</sub> using small amplitude flow oscillations. It allows the evaluation of several elementary kinetic parameters from one set of dynamic data for a reaction

mechanism based on a single catalytic site. The optimized transient model is able to reproduce the time-evolution of the reactant and product molar fractions at the outlet of a fixed bed operated with modulations of different amplitudes and frequencies. It further shows that the acetylene conversion is controlled by two steps, the hydrogen adsorption step and the hydrogenation of the surface vinyl intermediate into adsorbed ethylene.

## Introduction

More flexible reactor operation may be needed if excess renewable electricity is to be converted into chemical energy carriers or used for heating chemical processes.<sup>[1]</sup> Dynamic reactor operations will become more important to deal with the intermittent nature of electricity from renewable sources. For example, during peak hours, water electrolysis might be used to produce hydrogen that can be further stored in liquid organic hydrogen carriers. Or an endothermic process might be run in an electrically heated reactor. The use of renewable energy requires the reactor to run at various operating points, but still at steady-state. Transient operation only occurs when switching from one stationary point to the other. Dynamic reactor operation has been studied for the last decades,<sup>[2]</sup> mostly with the aim to enhance the performance with respect to the steady-state operation. Reaction kinetics are required for upscaling and reactor design, but steady-state kinetics are

inadequate for designing dynamic processes, as the individual steps such as adsorption, desorption and surface reactions all have different characteristic time constants.<sup>[3]</sup> Different experimental approaches to study transient kinetics have been developed. Transient experiments such as TAP, step-response and SSITKA give more detailed insights into reaction mechanisms than steady-state experimentation.<sup>[3–12]</sup> SSITKA experiments offer the advantage of containing dynamic information while the catalyst remains at steady-state.<sup>[5]</sup> Another possibility is to operate the reactor by concentration modulation around the steady-state. These types of experiments can be used for model discrimination and kinetic studies.<sup>[7–12]</sup> Additional information can be obtained by varying the frequency and performing a frequency analysis.

We here report on a simple method to perform these experiments and apply it to the investigation of the selective hydrogenation of acetylene over an alumina supported palladium catalyst. This provides for a more complex case than the adsorption experiments reported previously.<sup>[1,2]</sup>

Selective hydrogenation of acetylene is an important process in petrochemical industry to reduce the amount of acetylene present in the C<sub>2</sub> fraction of the steam cracker. The acetylene content is reduced from 0.8–1.6% to less than 5 or 1 ppm for chemical grade and polymer grade ethylene, respectively. Selective acetylene hydrogenation is operated in two different process configurations: front-end and tail-end.<sup>[13]</sup> The tail-end configuration represents 70% of all units worldwide. The process is placed after CH<sub>4</sub> and H<sub>2</sub> separation and hydrogen is added in a slightly higher amount than acetylene, while the majority of the stream contains ethylene.<sup>[13,14]</sup> Alumina-supported palladium or bimetallic palladium-silver catalysts are used for this process, assuring very high activity and selectivity for acetylene hydrogenation. The formation of C<sub>4</sub> byproducts is quite common under tail-end conditions as is the formation of coke causing catalyst deactivation.

Several studies report on the kinetics of this reaction<sup>[11,14–24]</sup> and the kinetics have been reviewed by Borodziński and

[a] Dr. C. Urmès, Dr. C. Daniel, Dr. Y. Schuurman  
IRCELYON

Université Lyon 1  
CNRS, UMR5256  
2 avenue Albert Einstein  
69626 Villeurbanne Cedex (France)  
E-mail: yves.schuurman@ircelyon.univ-lyon1.fr

[b] Dr. C. Urmès, Dr. J.-M. Schweitzer, Dr. A. Cabiac  
IFP Energies nouvelles  
Etablissement de Lyon  
Rond-point de l'échangeur de Solaize  
BP3, 69360 Solaize (France)

[c] Dr. C. Julcour  
Laboratoire de Génie Chimique  
Université de Toulouse, CNRS, INPT, UPS  
Toulouse (France)

 Supporting information for this article is available on the WWW under <https://doi.org/10.1002/cctc.202101826>

 This publication is part of a joint Special Collection with ChemElectroChem on "Catalysts and Reactors under Dynamic Conditions for Energy Storage and Conversion (DynaKat)". Please check the ChemCatChem homepage for more articles in the collection.

Bond.<sup>[20]</sup> The details of the reaction mechanism are still being debated. The most sophisticated models contain distinct sites, catalyzing specific reactions depending on the size of the site. Small sites favour adsorption and selective hydrogenation of acetylene to ethylene, whereas large sites are restricted to the adsorption of ethylene. Pachulski et al.<sup>[21]</sup> evaluated a large number of different rate equations for acetylene hydrogenation over Pd–Ag/Al<sub>2</sub>O<sub>3</sub>. They found that the best rate equation was based on two different sites. Our recent kinetic study under steady-state conditions over Pd/Al<sub>2</sub>O<sub>3</sub>, however, showed the most adequate rate equation to be based on a single site.<sup>[24]</sup> The data were compared to those of Borodziński and Cybulski,<sup>[16]</sup> and contrary to their study, an effect of the ethylene

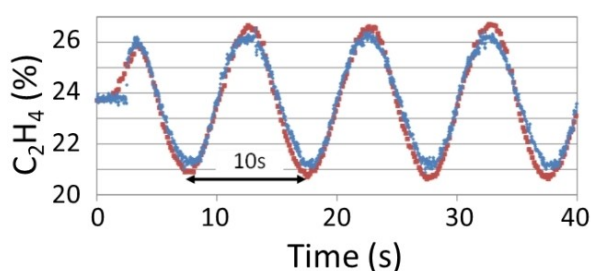


**Figure 1.** Ethylene molar fraction at the exit of a fixed bed reactor by modulated flow at 0.1 Hz. Square symbols: analysis by mass spectrometry, triangular symbols: analysis by FTIR spectroscopy.

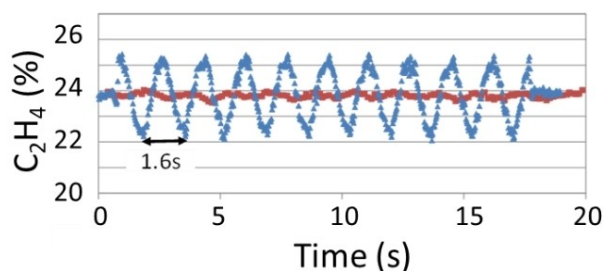


**Figure 2.** Ethylene molar fraction at the exit of a fixed bed reactor by modulated flow at 0.6 Hz. Square symbols: analysis by mass spectrometry, triangular symbols: analysis by FTIR spectroscopy.

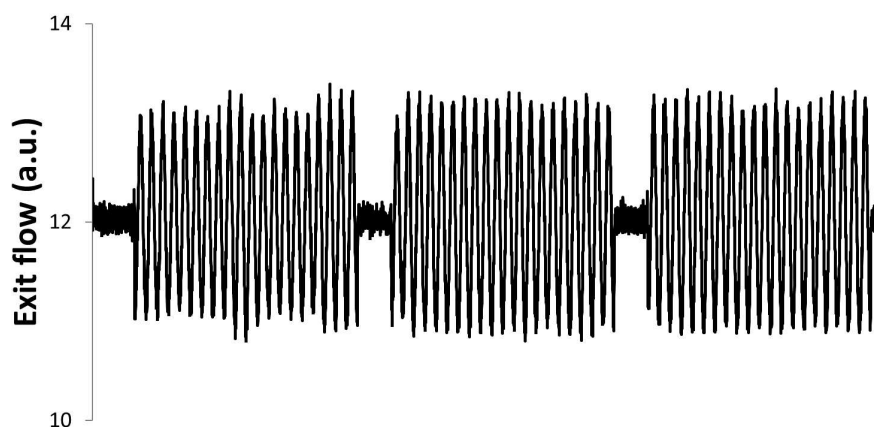
partial pressure on the acetylene hydrogenation rate was observed, indicating that a single site is sufficient. Cider and Schöön have studied the hydrogenation of acetylene in presence of carbon monoxide by transient pulse method.<sup>[11,17]</sup> They revisited the two-site model and concluded that there exists only one type of active sites for the reaction but two types of sites for acetylene adsorption during the cross-desorption of carbon monoxide.

## Results and Discussion

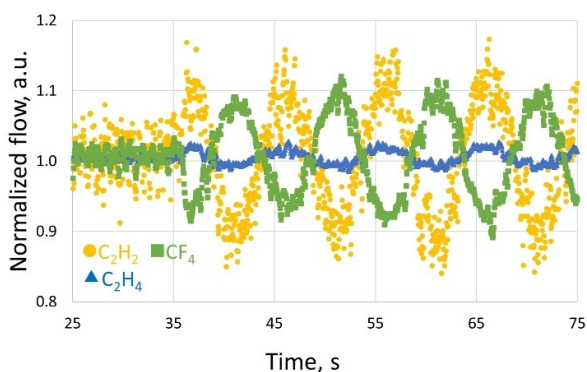
Initial flow modulation experiments were performed using an online mass spectrometer connected to the reactor outlet by a 1.5 m capillary. Figure 1 compares the ethylene outlet flow, measured by the mass spectrometer and the FTIR spectrometer using the small volume gas cell at a low modulation frequency of 0.1 Hz. A good agreement was obtained by both analyses. At a higher frequency of 0.6 Hz, as shown in Figure 2, the mass spectrometer signal was strongly attenuated, while the attenuation of the FTIR signal was in line with the expected loss due to the increasing frequency.<sup>[12]</sup> The mass spectrometer inlet capillary and inlet system act as a filter for the modulated signal. Therefore, no mass spectrometer analysis was used in this study. As a consequence, no hydrogen outlet flow could be measured, as hydrogen is not detected by the FTIR analysis.

Figure 3 shows the experimental protocol that was used for kinetic flow modulation experiments. After the steady-state was reached 20 oscillations were introduced, followed by a period at steady-state. This sequence was repeated 3 times. Figure 3 shows a good reproducibility of both the steady-state and the oscillations.

Figure 4 shows the outlet flows of tetrafluoromethane, acetylene and ethylene at 25 °C when no reaction takes place for an amplitude of 8.3%. The signals are normalized with respect to the mean molar flow. Therefore, the amplitudes of acetylene and ethylene are different. The amplitude of the ethylene signal is small, because of the large mean flow of ethylene fed to the reactor. The outlet flows of acetylene and ethylene are found in counter phase with the tetrafluoro-



**Figure 3.** Experimental procedure for flow modulated experiments. Outlet flow of tetrafluoromethane.



**Figure 4.** Outlet flows of tetrafluoromethane (■), acetylene (●) and ethylene (←) at 25 °C (no conversion). Frequency = 0.1 Hz, amplitude of 8.3%.

methane tracer flow as set for the inlet flows. Figure 5 shows the outlet flows of the mixture at 45 °C for the same amplitude. The formation of ethane can be observed in counter phase with the acetylene flow. This is due to the strong adsorption of acetylene, resulting in a negative reaction order. When the acetylene concentration is low, free sites are created where hydrogen can adsorb and react to produce ethane. Nievergeld showed this same phenomenon by simulations of a three-step reaction mechanism in a plug-flow reactor.<sup>[10]</sup>

In a previous study we have developed Langmuir-Hinshelwood rate equations based on a sequence of elementary steps

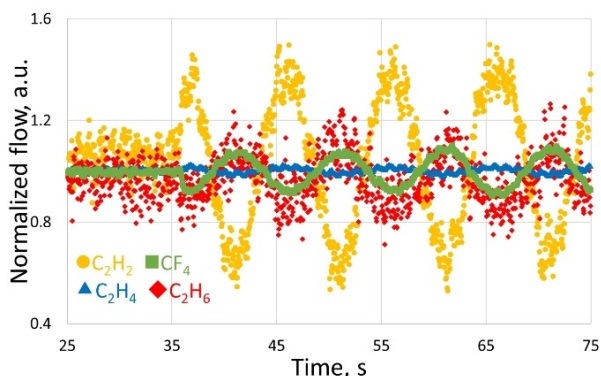


**Figure 5.** Outlet flows of tetrafluoromethane (■), acetylene (●), ethylene (←) and ethane (◆) at 45 °C. Frequency = 0.1 Hz, amplitude of 8.3%.

for the steady-state hydrogenation of acetylene.<sup>[12]</sup> The proposed reaction mechanism consists of a series of sequential hydrogen additions according to the Horiuti-Polanyi mechanism<sup>[22,31]</sup> and is given in Table 1. Dihydrogen adsorption takes place dissociatively on two free neighboring palladium surface atoms (step (1)). Acetylene adsorbs molecularly (step (2)). Adsorbed hydrogen and adsorbed acetylene react in step (4) to form a vinyl intermediate. This intermediate reacts further in step (5) with a second hydrogen atom to form adsorbed ethylene. Ethylene then either desorbs or reacts with adsorbed hydrogen to form an ethyl intermediate (step (3) or step (6)). This intermediate then forms ethane, which desorbs instantaneously, through the reaction with a second hydrogen atom (step (7)). Although a number of studies in the literature indicate that two distinct sites are involved in the hydrogenation of acetylene,<sup>[14,20,21]</sup> our kinetic data showed that an adequate description could be obtained by a reaction mechanism based on a single site, assumed to correspond to a surface palladium atom.<sup>[12]</sup>

A number of assumptions was needed to derive the Langmuir-Hinshelwood rate equations, such as the rate-determining step and the most abundant reactive intermediates. Here a microkinetic approach is used with no *a priori* assumption on the rate-determining step. The parameters for the elementary steps were estimated by regression analysis of the flow modulated transient data. Only the data at 0.1 Hz and amplitude of 8.3% at 45 °C were used for the parameter estimation. The three series of experiments (Figure 3) were averaged to increase the signal to noise ratio. The data at 0.5 Hz and amplitude of 25% at 45 °C were used for model validation. Initial parameter estimates were taken from the steady-state model.<sup>[12]</sup> Preliminary regression analysis showed that not all 14 rate constants of the proposed reaction mechanism could be estimated from a single data set simultaneously. Some steps are in quasi-equilibrium and in that case only the value of the ratio of the forward and reverse rate constants could be estimated and not the individual values. Steps (4) and (6) were found to be fast and strongly correlated with steps (5) and (7), respectively, in agreement with the steady-state analysis. The parameters that have been estimated by regression analysis are given in bold in Table 1, while the other parameters were fixed at the values given in this table. The parameter estimates are given with their 95% confidence intervals, which are roughly between 5–20%. A strong correlation coefficient was found for

**Table 1.** Proposed reaction mechanism and estimated parameters. The parameter values in bold have been estimated from the data set at 0.1 Hz and amplitude of 8.3% at 45 °C. The parameter values are given with their 95% confidence intervals.

N°	Elementary Step	$k_f$ [45 °C] $K_{ads}$ [45 °C]	$k_r$ [45 °C]	$r_f/r_r$	DRC <sub>C<sub>2</sub>H<sub>2</sub></sub> *	DRC <sub>C<sub>2</sub>H<sub>6</sub></sub> *
1	$H_2 + 2^* \rightleftharpoons 2H^*$	$(8.6 \pm 0.4) 10^5 Pa^{-1} s^{-1}$	$(3.5 \pm 0.7) 10^4 s^{-1}$	1.67	1.06	0.75
2	$C_2H_2 + ^* \rightleftharpoons C_2H_2^*$	$19.6 \pm 4.3 Pa^{-1}$		1.00	0.00	0.00
3	$C_2H_4^* \rightleftharpoons C_2H_4 + ^*$	$(2.9 \pm 0.2) 10^{-2} Pa^{-1}$		1.00	0.00	0.00
4	$C_2H_2^* + H^* \rightleftharpoons C_2H_3^* + ^*$	$1.0 10^{-4}$		1.00	0.00	0.00
5	$C_2H_3^* + H^* \rightleftharpoons C_2H_4^* + ^*$	$(2.8 \pm 0.1) 10^4 s^{-1}$	$1.0 10^4 s^{-1}$	2.05	0.70	0.02
6	$C_2H_4^* + H^* \rightleftharpoons C_2H_5^* + ^*$	$1.0 10^{-4}$		1.00	0.00	0.00
7	$C_2H_5^* + H^* \rightleftharpoons C_2H_6 + 2^*$	$(2.1 \pm 0.1) 10^5 s^{-1}$	$1.0 10^6 Pa^{-1} s^{-1}$	1.03	-0.05	0.01

\*DRC<sub>i</sub> : degree of rate control<sup>[32]</sup> of species i. Details are given in the supporting information.

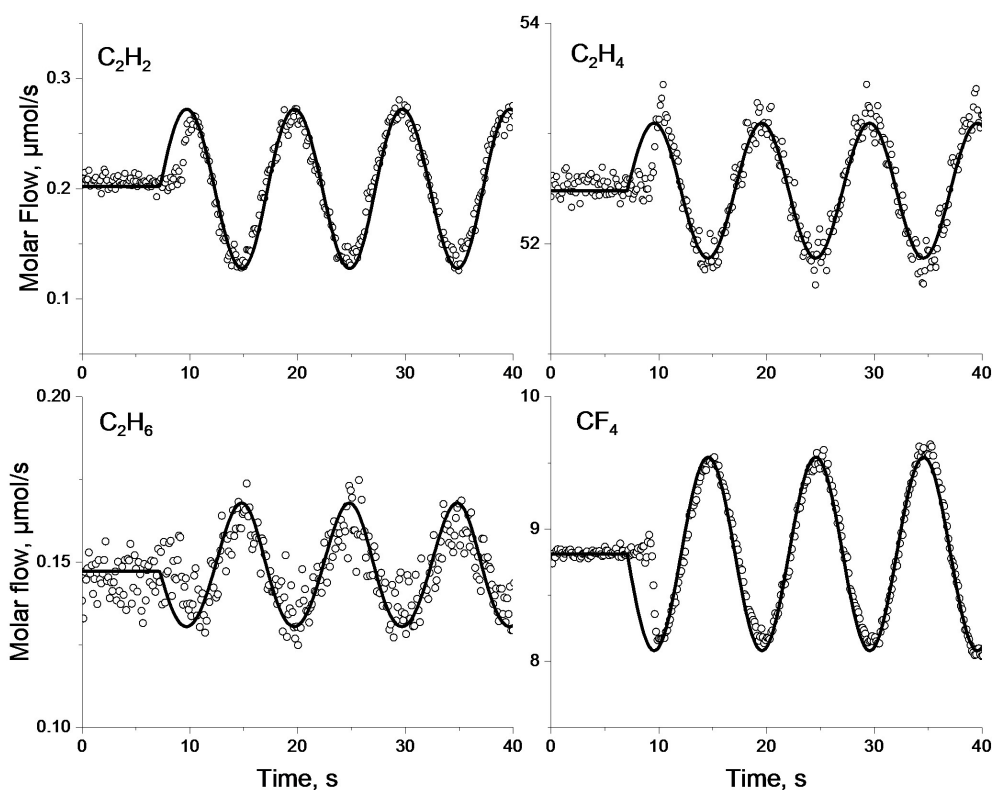
the hydrogen adsorption rate constant and the acetylene adsorption equilibrium constant. Fitting the data with a different value of the acetylene equilibrium adsorption constant resulted in a slightly higher residual sum of squares and different model responses for acetylene and ethane. Discrimination between the 2 parameter sets was not possible due to the too low signal to noise ratio. However, it is worth mentioning that although only a single transient data set was used for the regression analysis, much less correlation between the parameters was observed than for the steady-state study based on 69 experiments, resulting in a larger number of estimated parameters ( $t$ -values  $> 2$ ).

Figure 6 compares the model output with the experimental data for the responses of ethane, ethylene, acetylene and tetrafluoromethane. The model adequately describes the initial steady-state molar flows, as well as the periodic oscillations, but not the onset of the periodic operation. This is probably related to the start of the mass flow controllers as the tetrafluoromethane tracer shows a similar behavior. Figure S1 shows the data set at 0.5 Hz and an amplitude of 25% that were used as a validation set. Due to the larger amplitude, the perturbations lead to non-linearity and also very high acetylene conversion ( $\sim 90\%$ ) is reached, which leads to asymmetric oscillations. The model describes the asymmetric oscillations quite well for the ethane response, but slightly overestimates the acetylene oscillations. The larger amplitude leads to a larger variation of the surface coverages (Figure S2). Adsorption constants often

depend on the surface coverage and probably the model can be refined by taking this into account.

The micro-kinetic model was used to further explore the features of the mechanism. Table 1 lists the ratio of the forward and reverse rates,  $r_f/r_r$ , for each reaction step. Only three reaction steps (steps (1), (5)&(7)) are not in quasi-equilibrium, (e.g. the ratio,  $r_f/r_r$ , is not equal to 1). The same three steps also have non-zero values for the degree of rate control,  $DRC_{C_2H_2}$ , (see supporting information for more details) indicating that these steps have a direct effect on the overall rate.<sup>[32]</sup> The acetylene conversion is controlled especially by the hydrogen adsorption step (1) and the surface hydrogenation step of the vinyl species (step (5)). A change in the first step will lead to a change in the ethane production, but this is not the case for step (5) as shown by the degree of rate control for ethane (Table 1). Modifying the hydrogen adsorption kinetics can thus have an influence on the product selectivity.

The net rates for each step are depicted in Figure 7. The rate of steps (4), (5) and (6), (7) cannot be differentiated even under periodic operation, whereas the rate of acetylene adsorption coincides with the rates of steps (4), (5) under steady-state operation, but is slightly shifted under dynamic operation. The model can thus be simplified by lumping steps (4), (5) and (6), (7) into a single step each. This will eliminate the unknown parameters  $K_4$  and  $K_6$ . The net rate of step (3) is negative, because it has been written as an adsorption step in Table 1, while the net process is ethylene desorption.



**Figure 6.** Comparison of model predicted (solid lines) and experimental data (open symbols) for the flow modulated acetylene hydrogenation over Pd/ $\alpha$ -Al<sub>2</sub>O<sub>3</sub>.  $T = 45^\circ\text{C}$ , Frequency = 0.1 Hz, Amplitude of 8.3%.

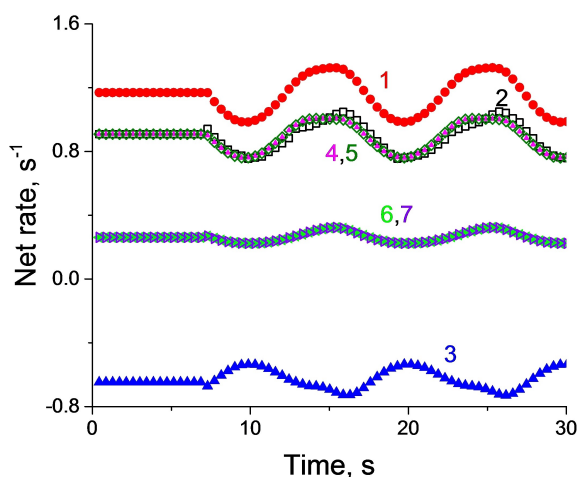


**Figure 7.** Calculated net rates for the steps in Table 1. Flow modulated acetylene hydrogenation over Pd/ $\alpha$ -Al<sub>2</sub>O<sub>3</sub>,  $T=45^\circ\text{C}$ , Frequency=0.1 Hz, Amplitude of 8.3%.

Figure 8 shows the surface coverages as calculated by the model. Adsorbed acetylene is the most abundant surface intermediate, followed by adsorbed ethylene. All other fractions of surface intermediates are at least an order of magnitude smaller. The fraction of free surface sites is very low, e.g.  $\theta_*$  equals approximately  $10^{-4}$ .

## Conclusions and Outlook

Dynamic reactor operations will be required to deal with the intermittent nature of electricity from renewable sources. Most catalyst performance testing and kinetic studies in the laboratory are carried out under steady-state conditions. Experimental rigs are nowadays equipped with digital mass flow controllers. By using an inexpensive data acquisition card

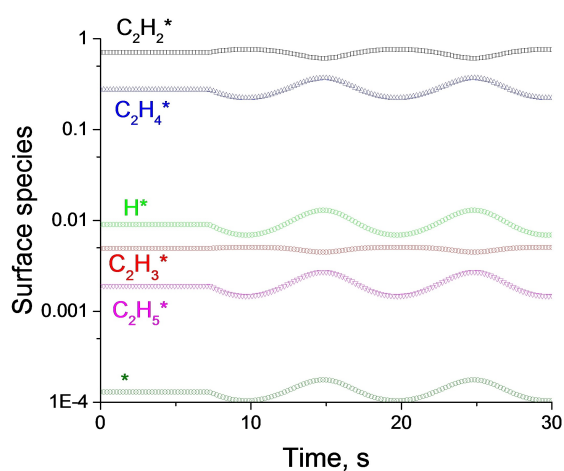


**Figure 8.** Calculated surface coverages for surface species in Table 1. Flow modulated acetylene hydrogenation over Pd/ $\alpha$ -Al<sub>2</sub>O<sub>3</sub>,  $T=45^\circ\text{C}$ , Frequency=0.1 Hz, Amplitude of 8.3%.

and a regular PC, the mass flow controllers can be set-up for flow modulation experiments. These experiments allow to study the catalysts dynamics and detailed kinetic studies. Dead volumes should be minimized and a proper time-resolved analysis is necessary. Here we used a fast FTIR spectrometer with a small volume gas cell that leads to very fast analysis times. Alternatively, a multiloop sample valve can be used combined with a regular GC analysis for experiments on a shorter timescale.<sup>[11]</sup>

A microkinetic model was developed for the selective hydrogenation of acetylene over Pd/Al<sub>2</sub>O<sub>3</sub>, consisting of a series of sequential hydrogen additions according to the Horvut-Polanyi mechanism. Parameter estimation was performed by regression analysis of flow modulated acetylene hydrogenation experiments. Several kinetically significant parameters could be obtained by regression analysis of the data at 0.1 Hz and 8.3% flow amplitude. The degree of rate control showed that the acetylene conversion is controlled by mainly 2 steps, the hydrogen adsorption step and the hydrogenation of the surface vinyl intermediate into adsorbed ethylene. The reaction mechanism contains only a single site where both the hydrogenation of acetylene and ethylene occur.

Experiments with larger amplitudes revealed that the reaction mechanism is more complex, probably due to the larger variation of surface coverages. Adsorption constants are often dependent on the surface coverage, which was not included in the model and requires additional parameters.

## Materials and Methods

### Catalyst

A 0.05 wt.% Pd/ $\alpha$ -alumina was used as a catalyst.  $\alpha$ -alumina beads of 2–3 mm were impregnated by an aqueous palladium nitrate solution. The beads were dried at 120 °C under air and calcined for 2 h at 425 °C. The catalyst was reduced at 150 °C for 2 h under a flow of 50 mL/min of 50% hydrogen in argon. The catalyst was then stabilized under reactive flow conditions at 50 °C for 4 h. After this period, the catalyst activity and selectivity were stable during the runs.

The detailed synthesis protocol has been described previously, providing extensive high-resolution transmission electron microscopy and X-ray diffraction analysis.<sup>[25,26]</sup> The  $\alpha$ -alumina support has a BET surface area of 10 m<sup>2</sup>/g and a porous volume of 0.54 mL/g. Electron transmission microscopy analysis showed a mean palladium particle diameter of  $2.4 \pm 0.7$  nm, corresponding to a dispersion of ca. 40%. The number of surface palladium atoms was calculated as  $N_s = 2 \times 10^{-3}$  mol/kg.

### Experimental set-up

All experiments were carried out in a fixed bed reactor, consisting of a steel tube with an inner diameter of 2.8 mm. 200 mg of crushed and sieved catalyst (100–200  $\mu\text{m}$ ) were used. By using appropriate criteria, the kinetic measurements at

steady-state conditions were shown to be free from heat and mass transfer limitations.<sup>[24]</sup> During the catalyst reduction the reactor was placed in a resistively heated furnace, while for the kinetic runs the reactor was immersed in a thermostatic water bath. Switching from one heating device to another was done under inert flow, without exposing the catalyst to air. No thermocouple was present in the reactor, as due to the low amplitude of the oscillations no significant temperature variation was expected. The reactor pressure was measured by a pressure transducer at the reactor inlet. Six mass flow controllers (MFC) were used to mix the inlet gases. Two of them were controlled by a 0–5 V signal generated from a computer-controlled data acquisition card by sending a sinusoidal wave to the mass flow controllers to enforce periodic operation. The set-point return was sent back to the card, so that the actual flow was monitored directly by the computer. A schematic of the set-up has been presented in.<sup>[12]</sup>

Typical operation consisted of setting initially the three mass flow controllers to a fixed set-point to operate the reactor under a steady flow. Then two mass flow controllers were subjected to counter-phase sinusoidal modulation at a desired amplitude and frequency for a fixed number of cycles, before getting back to steady flow. The counter-phase operation insured a constant flowrate at the reactor inlet and limited pressure fluctuations. Periodic operation consisted of mixing a steady flow of argon, ethylene and hydrogen with two sinusoidal modulated flows of tetrafluoromethane (tracer) and ethylene/acetylene mixture (95/5 % mol) oscillating in counter-phase with a mean flow rate of 12 mL/min each. Table 2 summarizes the inlet flow for each gas, the amplitude and the phase shift in case of modulation. Note that both a steady-state flow and superimposed modulated flow of ethylene were used to get a mean molar fraction corresponding to tail-end conditions. Two sets of amplitudes (8.3&25 %) were used.

The frequency of the sinusoidal flow was varied from 0.1 to 0.5 Hz. The tracer tetrafluoromethane is used to account for the hydrodynamics of the experimental set-up. It was assumed that tetrafluoromethane does not adsorb on the catalyst. Experiments were carried out at 25 (no conversion) and 45 °C.

Online analysis was done by online mass spectrometry and by passing the outlet gas flow through a small volume (120 µL) infrared gas cell connected to a high-speed Fourier-Transformed InfraRed (FTIR) spectrometer. The data acquisition rate of the infrared spectrometer was around 25 data points per second (25 Hz), depending on the selected resolution. The latter one was usually set to 8 cm<sup>-1</sup> to favor high acquisition rates necessary to correctly trace the transient data. Quantitative FTIR

analysis of acetylene, ethylene and ethane was carried out. No C4 products were observed. The carbon balance was closed within 5%.

## Modeling and parameter estimation

The transient model was based on a one-dimensional pseudo-homogeneous description of the fixed bed reactor, in agreement with the absence of mass and heat transfer limitations. A constant gas velocity was assumed and the reactor was supposed to operate isothermally.

The continuity equations are then given for the gas phase and adsorbed phase respectively as [Eq. (1) and (2)]:

$$\varepsilon_b \frac{\partial C_i}{\partial t} = -u_s \frac{\partial C_i}{\partial z} + D_{ax,i} \frac{\partial^2 C_i}{\partial z^2} - (1 - \varepsilon_b) L_t (k_{ads,i} P_{gas,i} \theta_i^{n_i} - k_{des,i} \theta_i^{n_i}) \quad (1)$$

$$\frac{\partial \theta_i}{\partial t} = \sum_j v_{ij} k_j P_{gas,i}^{m_j} \prod_j \theta_j^{n_j} \quad (2)$$

Where  $t$  is the time (s),  $z$  the reactor axial coordinate (m),  $u_s$  the superficial gas velocity (m<sub>g</sub><sup>3</sup>/m<sub>r</sub><sup>2</sup>/s),  $D_{ax}$  the axial dispersion coefficient (m<sub>g</sub><sup>3</sup>/m<sub>r</sub>/s),  $\varepsilon_b$  the bed void fraction (m<sub>g</sub><sup>3</sup>/m<sub>r</sub><sup>3</sup>),  $C_i$  the gas phase concentration of each species (mol/m<sub>g</sub><sup>3</sup>).  $L_t$  is the number of active sites per catalyst volume (mol/m<sub>cat</sub><sup>3</sup>),  $k_{ads,i}$  the adsorption rate constant for the gas phase species  $i$  (Pa<sup>-1</sup>s<sup>-1</sup>),  $k_{des,i}$  the desorption rate constant for the gas phase species  $i$  (s<sup>-1</sup>),  $P_{gas,i}$  the partial pressure of species  $i$  in the gas phase (Pa),  $\theta_i$  the fractional surface coverage by species  $i$ ,  $\theta_*$  the fraction of free sites,  $v_{ij}$  is the stoichiometric coefficient for species  $i$  in reaction  $j$  and  $m_j$ ,  $n_j$  the reaction orders in reaction  $j$ .  $n_i$  indicates the type of adsorption of species  $i$  ( $n_i=1$  : molecular /  $n_i=2$  : dissociative).  $m_j$  is equal to 1 for adsorption and equal to 0 for desorption or surface reactions.

The following initial and boundary conditions are applied for all gas phase species  $i$  [Eq. (3)–(5)]:

$$t = 0 \ \& \ 0 \leq z \leq L : C_i = 0 \ \& \ \theta_i = 0 \quad (3)$$

$$t > 0 \ \& \ z = 0 : C_i = C_i^0 + A C_i^0 \sin(2\pi f t + \varphi_i) \quad (4)$$

$$t > 0 \ \& \ z = L : \frac{dC_i}{dz} = 0 \quad (5)$$

Where  $L$  is the reactor length (m),  $A$  the amplitude of the oscillations,  $f$  the oscillation frequency (Hz),  $t$  the time (s) and  $\varphi_i$  the phase shift with  $\varphi_i=\pi$  for the reactant and  $\varphi_i=0$  for the tracer tetrafluoromethane. Furthermore, the ideal gas law was applied.

This set of partial differential equations was transformed into a set of ordinary differential equations by the methods of lines and integrated numerically using the ODEPACK library.<sup>[27]</sup> Equation (1) is the diffusion-convection equation with a reaction term. It is commonly used for tracer studies in packed bed reactors.<sup>[28]</sup> Due to the short catalyst bed, the axial dispersion

**Table 2.** Inlet flow composition for modulated kinetic experiments.

Gas	Mean inlet flow [mL min <sup>-1</sup> ]	Amplitude 8.3% [mL min <sup>-1</sup> ]	Amplitude 25% [mL min <sup>-1</sup> ]	Phase shift
CF <sub>4</sub>	12.0	± 1.0	± 3.0	0
Ar	14.1			
H <sub>2</sub>	3.3			
C <sub>2</sub> H <sub>2</sub>	0.6	± 0.05	± 0.15	π
C <sub>2</sub> H <sub>4</sub>	11.4	± 0.95	± 2.85	π
C <sub>2</sub> H <sub>4</sub>	58.6			

cannot be neglected. The axial dispersion coefficient was calculated by the correlation given in.<sup>[28]</sup>

A non-linear weighted least-square multi-response regression analysis has been performed by a Levenberg-Marquardt minimization algorithm to optimize elementary reaction rate constants (or corresponding equilibrium constants).<sup>[29,30]</sup> The molar outlet flow of acetylene and ethane have been used for the objective function. After regression analysis the t-test, the approximate 95% confidence intervals of the parameter estimates and binary correlation coefficients were determined (details are given in the Supporting Information).

## Conflict of Interest

The authors declare no conflict of interest.

## Data Availability Statement

The data that support the findings of this study are available from the corresponding author upon reasonable request.

**Keywords:** transient kinetics · flow modulation · kinetics · selective hydrogenation · Pd/Al<sub>2</sub>O<sub>3</sub>

- [1] K. Kalz, R. Kraehnert, M. Dvoyashkin, R. Dittmeyer, R. Gläser, U. Krewer, J.-D. Grunwaldt, *ChemCatChem* **2017**, *9*, 17–29.
- [2] P. Silveston, R. R. Hudgins, A. Renken, *Catal. Today* **1995**, *25*, 91–112.
- [3] R. J. Berger, F. Kapteijn, J. A. Moulijn, G. B. Marin, J. De Wilde, M. Olea, D. Chen, A. Holmen, L. Lietti, E. Tronconi, Y. Schuurman, *App. Catal. A: Gen.* **2008**, *342*, 3–28.
- [4] K. Morgan, N. Maguire, R. Fushimi, J. T. Gleaves, A. Goguet, M. P. Harold, E. V. Kondratenko, U. Menon, Y. Schuurman, G. S. Yablonsky, *Catal. Sci. Technol.* **2017**, *7*, 2416–2439.
- [5] L. Shannon, J. G. Goodwin, *Chem. Rev.* **1995**, *95*, 677–695.
- [6] A. Bundhoo, J. Schweicher, A. Frennet, N. Kruse, *J. Phys. Chem. C* **2009**, *113*, 10731–10739.
- [7] Y.-E. Li, D. Willcox, R. D. Gonzalez, *AIChE J.* **1989**, *35*, 423–428.
- [8] A. Lie, J. Hoebink, G. Marin, *Chem. Eng. J.* **1993**, *53*, 47–54.
- [9] A. R. Garayhi, F. J. Keil, *Chem. Eng. J.* **2001**, *82*, 329–346.
- [10] A. Nievergeld, *Automotive Exhaust Gas Conversion: Reaction Kinetics, Reactor Modelling and Control*. PhD Thesis. 1998, Technische Universiteit Eindhoven, The Netherlands.
- [11] L. Cider, N.-H. Schön, *Ind. Eng. Chem. Res.* **1991**, *30*, 1437–1443.
- [12] C. Urmes, J. Obeid, J.-M. Schweitzer, A. Cabiac, C. Julcour, Y. Schuurman, *Chem. Eng. Sci.* **2020**, *214*, 114544.
- [13] M. Derrien, *Stud. Surf. Catal.* **1986**, *27*, 613–666.
- [14] A. Borodzinski, G. C. Bond, *Catal. Rev.* **2006**, *48*, 91–144.
- [15] A. N. R. Bos, K. R. Westerterp, *Chem. Eng. Process.* **1993**, *32*, 1–7.
- [16] A. Borodzinski, A. Cybulski, *Appl. Catal. A* **2000**, *198*, 51–66.
- [17] L. Cider, N.-H. Schön, *Appl. Catal.* **1991**, *68*, 207–216.
- [18] A. N. R. Bos, E. S. Bootsma, F. Foeth, H. W. J. Sleyster, K. R. Westerterp, *Chem. Eng. Process.* **1993**, *32*, 53–63.
- [19] H. Molero, B. F. Bartlett, W. T. Tysøe, *J. Catal.* **1999**, *181*, 49–56.
- [20] A. Borodzinski, G. C. Bond, *Catal. Rev.* **2008**, *50*, 379–469.
- [21] A. Pachulski, R. Schödel, P. Claus, *Appl. Catal. A* **2012**, *445–446*, 107–120.
- [22] D. Mei, P. A. Sheth, M. Neurock, C. M. Smith, *J. Catal.* **2006**, *242*, 1–15.
- [23] M. Neurock, R. A. Van Santen, *J. Phys. Chem. B* **2000**, *104*, 11127–11145.
- [24] C. Urmès, J.-M. Schweitzer, A. Cabiac, Y. Schuurman, *Catalysts* **2019**, *9*, 180.
- [25] M. Ramos-Fernandez, L. Normand, L. Sorbier, *Oil Gas Sci. Technol.* **2007**, *62*, 101–113.
- [26] B. Didillon, E. Merlen, T. Pagès, D. Uzio, *Stud. Surf. Sci. Catal.* **1998**, *118*, 41–54.
- [27] A. C. Hindemarsch, “ODEPACK, A systematized collection of ODE solvers” Elsevier, **1983**.
- [28] J. M. P. Q. Delgado, *Heat Mass Transfer* **2006**, *42*, 279–310.
- [29] K. Levenberg, *Q. Appl. Math.* **1944**, *11*, 164–168.
- [30] D. W. Marquardt, *J. Soc. Ind. Appl. Math.* **1963**, *11*, 431–441.
- [31] I. Horiuti, M. Polanyi, *Trans. Faraday Soc.* **1934**, *30*, 1164–1172.
- [32] C. T. Campbell, *Top. Catal.* **1994**, *1*, 353–366.

Manuscript received: November 30, 2021

Revised manuscript received: February 8, 2022

Accepted manuscript online: February 14, 2022

Version of record online: March 11, 2022